

Explicit Diffusion of Gaussian Mixture Model Based Image Priors

Martin Zach
{martin.zach,

Thomas Pock
pock}@icg.tugraz.at

Erich Kobler
kobler@uni-bonn.de

Antonin Chambolle
antonin.chambolle@ceremade.dauphine.fr

February 17, 2023

Abstract

In this work we tackle the problem of estimating the density f_X of a random variable X by successive smoothing, such that the smoothed random variable Y fulfills $(\partial_t - \Delta_1)f_Y(\cdot, t) = 0$, $f_Y(\cdot, 0) = f_X$. With a focus on image processing, we propose a product/fields of experts model with Gaussian mixture experts that admits an analytic expression for $f_Y(\cdot, t)$ under an orthogonality constraint on the filters. This construction naturally allows the model to be trained simultaneously over the entire diffusion horizon using empirical Bayes. We show preliminary results on image denoising where our model leads to competitive results while being tractable, interpretable, and having only a small number of learnable parameters. As a byproduct, our model can be used for reliable noise estimation, allowing blind denoising of images corrupted by heteroscedastic noise.

1 Introduction

Consider the practical problem of estimating the probability density $f_X : \mathcal{X} \rightarrow \mathbb{R}$ of a random variable X in \mathcal{X} , given a set of data samples $\{x_i\}_{i=1}^N$ drawn from f_X .¹ This is a challenging problem in high dimension (e.g. for images of size $M \times N$, i.e. $\mathcal{X} = \mathbb{R}^{M \times N}$), due to extremely sparsely populated regions. A fruitful approach is to estimate the density at different times when undergoing a diffusion process. Intuitively, the diffusion equilibrates high- and low-density regions over time, thus easing the estimation problem.

Let Y_t (carelessly) denote the random variable whose distribution is defined by diffusing f_X for some time t . We denote the density of Y_t by $f_Y(\cdot, t)$, which fulfills the diffusion equation $(\partial_t - \Delta_1)f_Y(\cdot, t) = 0$, $f_Y(\cdot, 0) = f_X$. The empirical Bayes theory [12] provides a machinery for reversing the diffusion process: Given an instantiation of the random variable Y_t , the Bayesian least-squares estimate of X can be expressed solely using $f_Y(\cdot, t)$. Importantly,

¹For notational convenience, throughout this article we do not make a distinction between the *distribution* and *density* of a random variable.

this holds for all positive t , as long as f_Y is properly constructed.

In practice we wish to have a parametrized, trainable model of f_Y , say f_θ where θ is a parameter vector, such that $f_Y(x, t) \approx f_\theta(x, t)$ for all $x \in \mathcal{X}$ and all $t \in [0, \infty)$. Recent choices for the family of functions $f_\theta(\cdot, t)$ were of practical nature: Instead of an analytic expression for f_θ at any time t , authors proposed a time-conditioned network in the hope that it can learn to behave as if it had undergone a diffusion process. Further, instead of worrying about the normalization $\int_{\mathcal{X}} f_Y(\cdot, t) = 1$ for all $t \in [0, \infty)$, usually they directly estimate the *score* $-\nabla_1 \log f_Y(\cdot, t) : \mathcal{X} \rightarrow \mathcal{X}$ with some network $s_\theta(\cdot, t) : \mathcal{X} \rightarrow \mathcal{X}$. This has the advantage that normalization constants vanish, but usually, the constraint $\partial_j(s_\theta(\cdot, t))_i = \partial_i(s_\theta(\cdot, t))_j$ is not enforced in the architecture of s_θ . Thus, $s_\theta(\cdot, t)$ is in general not the gradient of a scalar function (the negative-log-density it claims to model).

In this paper, we pursue a more principled approach. Specifically, we leverage Gaussian mixture models to represent the popular product/field of experts model [5, 14] and show that under an orthogonality constraint of the associated filters, the diffusion of the model can be expressed analytically.

2 Background

In this section, we first emphasize the importance of the diffusion process in density estimation (and sampling) in high dimensions. Then, we detail the relationship between diffusing the density function, empirical Bayes, and denoising score matching [18].

2.1 Diffusion Eases Density Estimation and Sampling

Let f_X be a density on $\mathcal{X} \subset \mathbb{R}^d$. A major difficulty in estimating f_X with parametric models is that f_X is extremely sparsely populated in high dimensional spaces², i.e.,

²Without any reference to samples $x_i \sim f_X$, an equivalent statement may be that f_X is (close to) zero almost everywhere (in the layman —

$d \gg 1$. This phenomenon has many names, e.g. the curse of dimensionality or the manifold hypothesis [1]. Thus, the learning problem is difficult, since meaningful gradients are rare. Conversely, let us for the moment assume we have a model \tilde{f}_X that approximates f_X well. In general, it is still very challenging to generate a set of points $\{x_i\}_{i=1}^I$ such that we can confidently say that the associated empirical density $\frac{1}{I} \sum_{i=1}^I \delta(\cdot - x_i)$ approximates \tilde{f}_X . This is because, in general, there does not exist a procedure to directly draw from \tilde{f}_X , and (modern) Markov chain Monte Carlo (MCMC) relies on the estimated gradients of \tilde{f}_X and, in practice, only works well for unimodal distributions [17].

The isotropic diffusion process or heat equation

$$(\partial_t - \Delta_1)f(\cdot, t) = 0 \text{ with initial condition } f(\cdot, 0) = f_X \quad (1)$$

equilibrates the density in f_X , thus mitigating the challenges outlined above. Here, ∂_t denotes $\frac{\partial}{\partial t}$ and $\Delta_1 = \text{Tr}(\nabla_1^2)$ is the Laplace operator, where the 1 indicates application to the first argument. We detail the evolution of f_X under this process and relations to empirical Bayes in Section 2.2.

Learning $f(\cdot, t)$ for $t \geq 0$ is more stable since the diffusion “fills the space” with meaningful gradients [16]. Of course, this assumes that for different times t_1 and t_2 , the models of $f(\cdot, t_1)$ and $f(\cdot, t_2)$ are somehow related to each other. As an example of this relation, the recently popularized noise-conditional score-network [17] shares convolution filters over time, but their input is transformed with a time-conditional instance normalization. In this work, we make this relation explicit by considering a family of functions $f(\cdot, 0)$ for which $f(\cdot, t)$ can be expressed analytically.

For *sampling*, $f(\cdot, t)$ for $t > 0$ can help by gradually moving samples towards high-density regions of f_X , regardless of initialization. To utilize this, a very simple idea with relations to simulated annealing [7, 17] is to have a pre-defined time schedule $t_T > t_{T-1} > \dots > t_1 > 0$ and sample $f(\cdot, t_i)$, $i = T, \dots, 0$ (e.g. with Langevin dynamics [13]) successively.

2.2 Diffusion, Empirical Bayes, and Denoising Score Matching

In this section, similar to the introduction, we again adopt the interpretation that the evolution in Eq. (1) defines the density of a smoothed random variable Y_t . That is, Y_t is a random variable with probability density $f_Y(\cdot, t)$, which fulfills $(\partial_t - \Delta_1)f_Y(\cdot, t) = 0$ and $f_Y(\cdot, 0) = f_X$. It is well known that the Green’s function of Eq. (1) is a Gaussian (see e.g. [2]) with zero mean and variance $\sigma^2(t) = 2t\text{Id}$. In other words, for $t > 0$ we can write $f_Y(\cdot, t) = G_{0,2t\text{Id}} * f_X$, where

$$G_{\mu, \Sigma}(x) = |2\pi\Sigma|^{-1/2} \exp\left(-\frac{1}{2}(x - \mu)^\top \Sigma^{-1}(x - \mu)\right). \quad (2)$$

Thus, the diffusion process constructs a (linear) *scale space in the space of probability densities*. In terms of the random not measure theoretic — sense).

variables, $Y_t = X + \sqrt{2t}N$ where $N \sim \mathcal{N}(0, \text{Id})$. We next motivate how to estimate the corresponding instantiation of X which has “most likely” spawned an instantiation of Y_t using empirical Bayes.

In the school of empirical Bayes [12], we try to estimate a clean random variable given a corrupted instantiation, using only knowledge about the corrupted density. In particular, for our setup, Miyasawa [9] has shown that the Bayesian least-squares estimator x_{EB} for an instantiation y_t of Y_t is

$$x_{\text{EB}}(y_t) = y_t + \sigma^2(t)\nabla_1 \log f_Y(y_t, t), \quad (3)$$

which is also known as Tweedie’s formula [3]. Raphan and Simoncelli [11] extended the empirical Bayes framework to arbitrary corruptions and coined the term non-parametric empirical Bayes least-squares (NEBLS).

Recently, Eq. (3) has been used frequently for parameter estimation in diffusion-based models. Let $\{x_i\}_{i=1}^I$ be a dataset of I samples drawn from f_X and Y_t governed by the considered diffusion process. Thus, both the left- and right-hand side of Eq. (3) are *known* — in expectation. This naturally leads to the loss function

$$\min_{\theta} \int_{(0, \infty)} \mathbb{E}_{(x, y_t) \sim f_X \times Y_t} \|x - y_t - \sigma(t)^2 \nabla_1 \log f_{\theta}(y_t, t)\| dt \quad (4)$$

for estimating θ such that $f_{\theta} \approx f_Y$. Here, $f_{X \times Y_t}$ denotes the joint distribution of real and degraded points. This learning problem is known as denoising score matching [6, 17, 18].

3 Methods

In this section, we introduce a patch and convolutional model to approximate the prior distribution of natural images. For both models, we present conditions such that they obey the diffusion process.

3.1 Patch Model

Patch-based prior models such as expected patch log likelihood (EPLL) [19] typically use Gaussian mixture models (GMMs) to approximately learn a prior for natural image patches. Throughout this section, we approximate the density of image patches $p \in \mathbb{R}^a$ of size $a = b \times b$ as a product of GMM experts, i.e.

$$\tilde{f}_{\theta}(p, t) = Z(\{k_j\}_{j=1}^J)^{-1} \prod_{j=1}^J \psi_j(\langle k_j, p \rangle, w_j, t), \quad (5)$$

in analogy to the product-of-experts model [5]. $Z(\{k_j\}_{j=1}^J)$ is required such that \tilde{f}_{θ} is properly normalized. Every expert $\psi_j : (\mathbb{R} \times \Delta^L \times [0, \infty)) \rightarrow \mathbb{R}^+$ for $j = 1, \dots, J$ models the density of associated filters k_j for all diffusion times t by an one-dimensional GMM with L components of the form

$$\psi_j(x, w_j, t) = \sum_{l=1}^L w_{jl} G_{\mu_l, \sigma_j^2(t)}(x). \quad (6)$$

The weights of each expert $w_j = (w_{j1}, \dots, w_{jL})^\top$ must satisfy the unit simplex constraint, i.e., $w_j \in \Delta^L$, $\Delta^L = \{x \in \mathbb{R}^L : x_l \geq 0, \sum_{l=1}^L x_l = 1\}$. Although not necessary, we assume for simplicity that all ψ_j have the same number of components and each component has the same mean. The discretization of μ_l over the real line is fixed a priori in a uniform way and detailed in Section 4.1. Further, the variances of all components of each expert are shared and are modeled as

$$\sigma_j^2(t) = \sigma_0^2 + c_j 2t,$$

where σ_0 is chosen to support the uniform discretization of the means μ_l and $c_j \in \mathbb{R}_{++}$ are constants, to reflect the convolution effect of the diffusion process.

Next, we show how the diffusion process leads to the linear change of each expert's variance $\sigma_j^2(t)$. In detail, we exploit two well-known properties of GMMs: First, the product of GMMs is again a GMM, see e.g. [15]. This allows us to work on highly expressive models that enable efficient *evaluations* due to factorization. Second, we use the fact that there exists an analytical solution to the diffusion equation if f_X is a GMM: The Green's function is a Gaussian with isotropic covariance $2t\text{Id}$. Hence, diffusion amounts to the convolution of two Gaussians for every component due to the linearity of convolution. Using previous notation, if X is a random variable with normal distribution $\mathcal{N}(\mu_X, \Sigma_X)$, then Y_t follows the distribution $\mathcal{N}(\mu_X, \Sigma_X + 2t\text{Id})$. In particular, the mean remains unchanged, thus it is sufficient to only adapt the variances in Eq. (5) linearly along with the diffusion time.

Theorem 1. $\tilde{f}(\cdot, 0)$ is a homoscedastic GMM on \mathbb{R}^a with L^J components, precision matrix

$$(\Sigma_a)^{-1} = \frac{1}{\sigma_0^2} \sum_{j=1}^J (k_j \otimes k_j). \quad (7)$$

and means $\mu_{a,\hat{i}} = \Sigma_a \sum_{j=1}^J k_j \mu_{\hat{i}(j)}$.

Proof. By definition,

$$\prod_{j=1}^J \psi(\langle k_j, p \rangle, w_j, 0) = \prod_{j=1}^J \sum_{l=1}^L \frac{w_{jl}}{\sqrt{2\pi\sigma_0^2}} \exp\left(-\frac{1}{2\sigma_0^2} (\langle k_j, p \rangle - \mu_l)^2\right). \quad (8)$$

Let $\hat{l}(j)$ be a fixed but arbitrary selection from the index set $\{1, \dots, L\}$ for each $j \in \{1, \dots, J\}$. The general component of the above reads as

$$(2\pi\sigma_0^2)^{-\frac{J}{2}} \left(\prod_{j=1}^J w_{j\hat{l}(j)} \right) \exp\left(-\frac{1}{2\sigma_0^2} \sum_{j=1}^J (\langle k_j, p \rangle - \mu_{\hat{l}(j)})^2\right). \quad (9)$$

To find $(\Sigma_a)^{-1}$, we complete the square as follows: Motivated by $\nabla_p \|p - \mu_a\|_{\Sigma_a^{-1}}^2 / 2 = \Sigma_a^{-1} (p - \mu_a)$ we find

$\nabla_p \left(\frac{1}{2\sigma_0^2} \sum_{j=1}^J (\langle k_j, p \rangle - \mu_{\hat{l}(j)})^2 \right) = \frac{1}{\sigma_0^2} \sum_{j=1}^J (k_j \otimes k_j) p - k_j \mu_{\hat{l}(j)}$ and the theorem immediately follows. \square

To get a tractable analytical expression for the diffusion process, we assume that the filters k_j are pairwise orthogonal, i.e. for all $i, j \in \{1, \dots, J\}$

$$\langle k_j, k_i \rangle = \begin{cases} 0 & \text{if } i \neq j, \\ \|k_j\|^2 & \text{else.} \end{cases} \quad (10)$$

Theorem 2 (Patch diffusion). *Under assumption Eq. (10), $\tilde{f}(\cdot, t)$ satisfies the diffusion equation $(\partial_t - \Delta_1)\tilde{f}(\cdot, t) = 0$ if $\sigma_j^2(t) = \sigma_0^2 + \|k_j\|^2 2t$.*

Proof. Assuming Eq. (10), the Eigendecomposition of the precision matrix can be trivially constructed. In particular, $(\Sigma_a)^{-1} = \sum_{j=1}^J \frac{\|k_j\|^2}{\sigma_0^2} \left(\frac{k_j}{\|k_j\|} \otimes \frac{k_j}{\|k_j\|} \right)$, hence $\Sigma_a = \sum_{j=1}^J \frac{\sigma_0^2}{\|k_j\|^2} \left(\frac{k_j}{\|k_j\|} \otimes \frac{k_j}{\|k_j\|} \right)$. As discussed in Section 2.2, Σ_a evolves as $\Sigma_a \mapsto \Sigma_a + 2t\text{Id}_a$ under diffusion. Equivalently, for all $j = 1, \dots, J$ Eigenvalues, $\frac{\sigma_0^2}{\|k_j\|^2} \mapsto \frac{\sigma_0^2 + 2t\|k_j\|^2}{\|k_j\|^2}$. Recall that σ_0^2 is just $\sigma_j^2(0)$. Thus, $\tilde{f}(\cdot, t)$ satisfies the diffusion equation if $\sigma_j^2(t) = \sigma_0^2 + \|k_j\|^2 2t$. \square

Corollary 2.1. *With assumption (10) the potential functions $\psi_j(\cdot, w_j, t)$ in Eq. (5) model the marginal distribution of the random variable $Z_{j,t} = \langle k_j, Y_t \rangle$. In addition, Eq. (5) is normalized when $Z(\{k_j\}_{j=1}^J)^{-1} = \prod_{j=1}^J \|k_j\|^2$.*

Proof. Consider one component of the resulting homoscedastic GMM: $\hat{Y}_t \sim \mathcal{N}(\mu_{a,\hat{i}}, \Sigma_a + 2t\text{Id}_a)$. The distribution of $\hat{Z}_{j,t} = \langle k_j, \hat{Y}_t \rangle$ is (see e.g. [4] for a proof) $\hat{Z}_{j,t} \sim \mathcal{N}(k_j^\top \mu_{a,\hat{i}}, k_j^\top (\Sigma_a + 2t\text{Id}_a) k_j) = \mathcal{N}(\mu_{\hat{l}(j)}, \sigma_0^2 + 2t\|k_j\|^2)$. The claim follows from the linear combination the different components. \square

We note that Eq. (7) only specifies a covariance matrix if $J = a$, otherwise the matrix is singular. In the case $J < a$, we restrict the analysis to the subspace $\text{span}(\{k_1, \dots, k_J\})$. In particular, we also assume that the diffusion process does not transport density out of this subspace.

3.2 Convolutional Model

To avoid the extraction and combination of patches in patch-based image priors and still account for the local nature of low-level image features, we describe a convolutional Gaussian mixture diffusion model (GMDM) next. The following analysis assumes vectorized images $x \in \mathbb{R}^n$ with n pixels; the generalization to higher dimensions is straightforward. In analogy to the patch-based model of the previous section, we extend the fields-of-experts model [14] to our considered diffusion setting by accounting for the diffusion time t and

obtain³

$$f_\theta(x, t) = \prod_{i=1}^n \prod_{j=1}^J \psi_j((K_j x)_i, w_j, t). \quad (11)$$

Here, each expert ψ_j models the density of convolution features extracted by convolution kernels $\{k_j\}_{j=1}^J$ of size $a = b \times b$. $\{K_j\}_{j=1}^J \subset \mathbb{R}^{n \times n}$ are the corresponding matrix representations and all convolutions are cyclic, i.e., $K_j x \equiv k_j *_n x$, where $*_n$ denotes a 2-dimensional convolution with cyclic boundary conditions. Further, $w_j \in \Delta^L$ are used to weight the components of each expert ψ_j as in Eq. (6). As in the patch model, it is sufficient to adapt the variances $\sigma_j^2(t)$ by the diffusion time as the following analysis shows.

By definition for $t = 0$, we have

$$f_\theta(x, 0) = \prod_{i=1}^n \prod_{j=1}^J \sum_{l=1}^L \frac{w_{jl}}{\sqrt{2\pi\sigma_0^2}} \exp\left(-\frac{((K_j x)_i - \mu_l)^2}{2\sigma_0^2}\right). \quad (12)$$

First, we expand the product over the pixels

$$f_\theta(x, 0) = \prod_{j=1}^J \sum_{\hat{l}(i)=1}^{L^n} (2\pi\sigma_0^2)^{-\frac{n}{2}} \bar{w}_{j\hat{l}(i)} \exp\left(-\frac{\|(K_j x) - \mu_{\hat{l}(i)}\|^2}{2\sigma_0^2}\right) \quad (13)$$

using the index map $\hat{l}(i)$ and $\bar{w}_{j\hat{l}(i)} = \prod_{i=1}^I w_{j\hat{l}(i)}$. Further, expanding over the features results in

$$f_\theta(x, 0) = \sum_{i(i,j)=1}^{(L^n)^J} (2\pi\sigma_0^2)^{-\frac{nJ}{2}} \bar{\bar{w}}_{i(i,j)} \exp\left(-\frac{1}{2\sigma_0^2} \sum_{j=1}^J \|(K_j x) - \mu_{i(i,j)}\|^2\right), \quad (14)$$

where $\bar{\bar{w}}_{i(i,j)} = \prod_{j=1}^J \prod_{i=1}^I w_{i(i,j)}$. Observe that Eq. (14) again describes a homoscedastic GMM with precision $\Sigma^{-1} = \frac{1}{\sigma_0^2} \sum_{j=1}^J K_j^\top K_j$ and means $\bar{\mu}_{i(i,j)} = \Sigma \frac{1}{\sigma_0^2} \sum_{j=1}^J K_j^\top \mu_{i(i,j)}$. Due to the assumed boundary conditions, the Fourier transform diagonalizes the convolution matrices: $K_j = F^* \text{diag}(F k_j) F$. Thus, the precision matrix can be expressed as

$$\Sigma^{-1} = F^* \text{diag}\left(\sum_{j=1}^J \frac{|F k_j|^2}{\sigma^2}\right) F \quad (15)$$

where we used $FF^* = \text{Id}$, $\bar{z}z = |z|^2$ and $|\cdot|$ denotes the complex modulus acting element-wise on its argument. We assume that the spectra of k_j have disjoint support, i.e.

$$\Gamma_i \cap \Gamma_j = \emptyset \quad \text{if } i \neq j, \quad (16)$$

³For simplicity, we discard the normalization constant Z , which is independent of t .

where $\Gamma_j = \text{supp } F k_j$. Note that, in analogy to the pair-wise orthogonality of the filters in the patch model Eq. (10), from this immediately follows that $\langle F k_j, F k_i \rangle = 0$ when $i \neq j$. In addition, we assume that the magnitude is constant over the support, i.e.

$$|F k_j| = \xi_j \mathbb{1}_{\Gamma_j}, \quad (17)$$

where $\mathbb{1}_A$ is the characteristic function of the set A .

Theorem 3 (Convolutional Diffusion). *Under assumptions (16) and (17), $f(\cdot, t)$ satisfies the diffusion equation $(\partial_t - \Delta_1)f(\cdot, t) = 0$ if $\bar{\sigma}_j^2(t) = \sigma_0^2 + \xi_j^2 2t$.*

Proof. The proof is in analogy to Theorem 2. By Eq. (15), under diffusion, $F^* \text{diag}\left(\sum_{j=1}^J \frac{\sigma^2}{|F k_j|^2}\right) F \mapsto F^* \text{diag}\left(\frac{\sigma^2 + 2t \sum_{j=1}^J |F k_j|^2}{\sum_{j=1}^J |F k_j|^2}\right) F$. Using Eq. (16) the inner sum decomposes as

$$\frac{\sigma_0^2 + 2t \sum_{j=1}^J |F k_j|^2}{\sum_{j=1}^J |F k_j|^2} = \sum_{j=1}^J \frac{\sigma_0^2 + 2t |F k_j|^2}{|F k_j|^2} \quad (18)$$

and with Eq. (17) the numerator reduces to $\sigma_0^2 + 2t \xi_j^2$. \square

4 Numerical Results

4.1 Numerical Optimization

For all experiments, ψ_j is a $L = 125$ component GMM, with equidistant means μ_l in the interval $[-\gamma, \gamma]$, where we chose $\gamma = 1$. To support the uniform discretization of the means, the shared standard deviation of the experts is $\sigma_0 = \frac{2\gamma}{L-1}$. Assuming zero-mean filters of size $b \times b$, we use $J = b^2 - 1$ filters. Each component of the initial filters is independently drawn from a zero-mean Gaussian distribution with standard deviation b^{-1} . We avoid simplex projections by replacing w_j with learnable parameters ζ_j , from which w_j are computed using a soft-argmax $w_{jl} = \frac{\exp \zeta_{jl}}{\sum_{l=1}^L \exp \zeta_{jl}}$, and initialize $\zeta_{jl} = \frac{0.1\sqrt{\alpha}}{1 + \alpha \mu_l^2}$, where $\alpha = 1000$.

For the numerical experiments, f_X reflects the distribution of rotated and flipped $b \times b$ patches from the 400 gray-scale images in the BSDS 500 [8] training and test set, with each pixel in the interval $[0, 1]$. We optimize the parameters $\theta = \{(k_j, \zeta_j)\}_{j=1}^J$ in Eq. (4) using the iPALM algorithm [10] with respect to a randomly chosen batch of size 3200 for 100 000 steps. We approximate the infinite-time diffusion process by uniformly drawing $\sqrt{2t}$ from the interval $[0, 0.4]$. We detail how we ensure the orthogonality of the filters during the iterations of iPALM in the next section.

4.1.1 Enforcing Orthogonality

Let $K = [k_1, k_2, \dots, k_J] \in \mathbb{R}^{a \times J}$ denote the matrix obtained by horizontally stacking the filters. We are interested in finding

$$\text{proj}_{\mathcal{O}}(K) = \arg \min_{M \in \mathcal{O}} \|M - K\|_F^2 \quad (19)$$

where $\mathcal{O} = \{X \in \mathbb{R}^{a \times J} : X^\top X = D^2\}$, $D = \text{diag}(\lambda_1, \lambda_2, \dots, \lambda_J)$ is diagonal, and $\|\cdot\|_F$ is the Frobenius norm. Since $\text{proj}_{\mathcal{O}}(K)^\top \text{proj}_{\mathcal{O}}(K) = D^2$ we can represent it as $\text{proj}_{\mathcal{O}}(K) = OD$ with O semi-unitary ($O^\top O = \text{Id}$). Other than positivity, we do not place any restrictions on $\lambda_1, \dots, \lambda_J$, as these are related to the precision in our model. Thus, we rewrite the objective

$$\begin{aligned} \text{proj}_{\mathcal{O}}(K) = & \arg \min_{\substack{O^\top O = \text{Id}_J \\ D = \text{diag}(\lambda_1, \dots, \lambda_J)}} \\ \{ \|OD - K\|_F^2 = & \|K\|_F^2 - 2\langle K, OD \rangle_F + \|D\|_F^2 \} \end{aligned} \quad (20)$$

where $\langle \cdot, \cdot \rangle_F$ is the Frobenius inner product.

We propose the following alternating minimization scheme for finding O and D . The solution for the reduced sub-problem in O can be computed by setting $O = U$, using the polar decomposition of $DK^\top = UP$, where $U \in \mathbb{R}^{J \times a}$ is semi-unitary ($U^\top U = \text{Id}_a$) and $P = P^\top \in \mathbb{S}_+^a$. The sub-problem in D is solved by setting $D_{i,i} = ((O^\top K)_{i,i})_+$. The algorithm is summarized in Algorithm 1, where we have empirically observed fast convergence; $B = 3$ steps already yielded satisfactory results. A theoretical analysis of the algorithm is presented in the supplemental material.

Algorithm 1: Algorithm for orthogonalizing a set of filters K .

Input : $K = [k_1, \dots, k_J] \in \mathbb{R}^{a \times J}$, $B \in \mathbb{N}$,
 $D^{(1)} = \text{Id}_J$
Output : $O^{(B)} D^{(B)} = \text{proj}_{\mathcal{O}}(K)$
1 for $b \in 1, \dots, B - 1$ **do**
2 $U^{(b)} P^{(b)} = D^{(b)} K^\top$ // Polar decomposition
3 $O^{(b+1)} = U^{(b)}$
4 $D_{i,i}^{(b+1)} = (((O^{(b+1)})^\top K)_{i,i})_+$

To visually evaluate whether our learned model matches the empirical marginal densities for any diffusion time t , we plot them in Fig. 1. At the top, the learned 7×7 orthogonal filters k_j are depicted, the associated learned potential functions $-\log \psi_j$ are shown below. Indeed, they match the empirical marginal responses

$$h_j(z, t) = -\log \mathbb{E}_{p \sim f_X} \delta(z - \langle k_j, p \rangle) \quad (21)$$

visualized at the bottom almost perfectly even at the low-density tails. In accordance to Theorem 2, the potentials barely change with t when $\|k_j\|$ is small. Conversely, when $\|k_j\|$ is large, the change is much more drastic. We observe the same for 15×15 filters, as shown in the supplementary material.

4.2 Sampling

A direct consequence of Corollary 2.1 is that our model admits a simple sampling procedure: The statistical independence of the components allows to draw random patches

by $Y_t = \sum_{j=1}^J \frac{k_j}{\|k_j\|^2} Z_{j,t}$, where $Z_{j,t}$ is sampled from the one-dimensional GMM ψ_j . The samples in Fig. 2 indicate a good match over a wide range of t . However, for small t the generated patches appear slightly noisy, which is due to an over-smooth approximation of the sharply peaked marginals around 0.

4.3 Image Denoising

For the denoising experiments, we use the 68 test images from [8]. To exploit our prior for denoising, we employ empirical Bayes-patch averaging (EB-PA) and the half-quadratic splitting (HQS) algorithm [19]. In HQS, we approximate the solution to the inner MAP problem with one empirical Bayes step on $\tilde{f}_\theta(\cdot, t)$, and set $\beta = \frac{1}{2t}$ for using a predefined schedule for t . The quantitative analysis in Table 1 shows competitive performance, especially given the relatively small number of parameters in our model.

4.4 Noise Estimation and Blind Image Denoising

The construction of our model allows us to interpret $\tilde{f}_\theta(\cdot, t)$ as a time-conditional likelihood density. Fig. 3 shows that we can utilize our model for heteroscedastic blind denoising, by estimating pixel-wise noise and using EB-PA. Fig. 4 shows the expected negative-log density over a range of σ and $\sqrt{2t}$. For visualization purposes, we normalized the negative-log density to have a minimum of zero over t : $l_\theta(x, t) = -\log \tilde{f}_\theta(x, t) - (\max_t \log \tilde{f}_\theta(x, t))$. The estimate $\sigma \mapsto \arg \min_t \mathbb{E}_{p \sim f_X, \eta \sim \mathcal{N}(0, \text{Id})} l_\theta(p + \sigma \eta, t)$ is a very good match to $\sigma \mapsto \sqrt{2t}$.

5 Conclusion

In this paper, we introduced GMDMs as products of GMMs on filter responses that allow for an explicit solution of the diffusion equation of the associated density. Our explicit formulation enables learning of product/field-of-experts-like image priors simultaneously for all diffusion times using denoising score matching. Our numerical results demonstrated that GMDMs capture the statistics of natural image patches well for any noise level and hence are suitable for heteroscedastic (blind) image denoising. In future work, we plan to extend the numerical evaluation to the convolutional model and apply our framework to challenging inverse problems in medical imaging.

A Preliminary Theoretical Analysis of Projection Algorithm

The problem is given $K \in \mathbb{R}^{m \times n}$, $n \leq m$, find $A \in \mathbb{R}^{m \times n}$ such that $A^\top A$ is a diagonal $n \times n$ matrix which minimizes $\|A - K\|_2$. We decompose $K = U^K \Sigma^K (V^K)^\top$ and $A =$

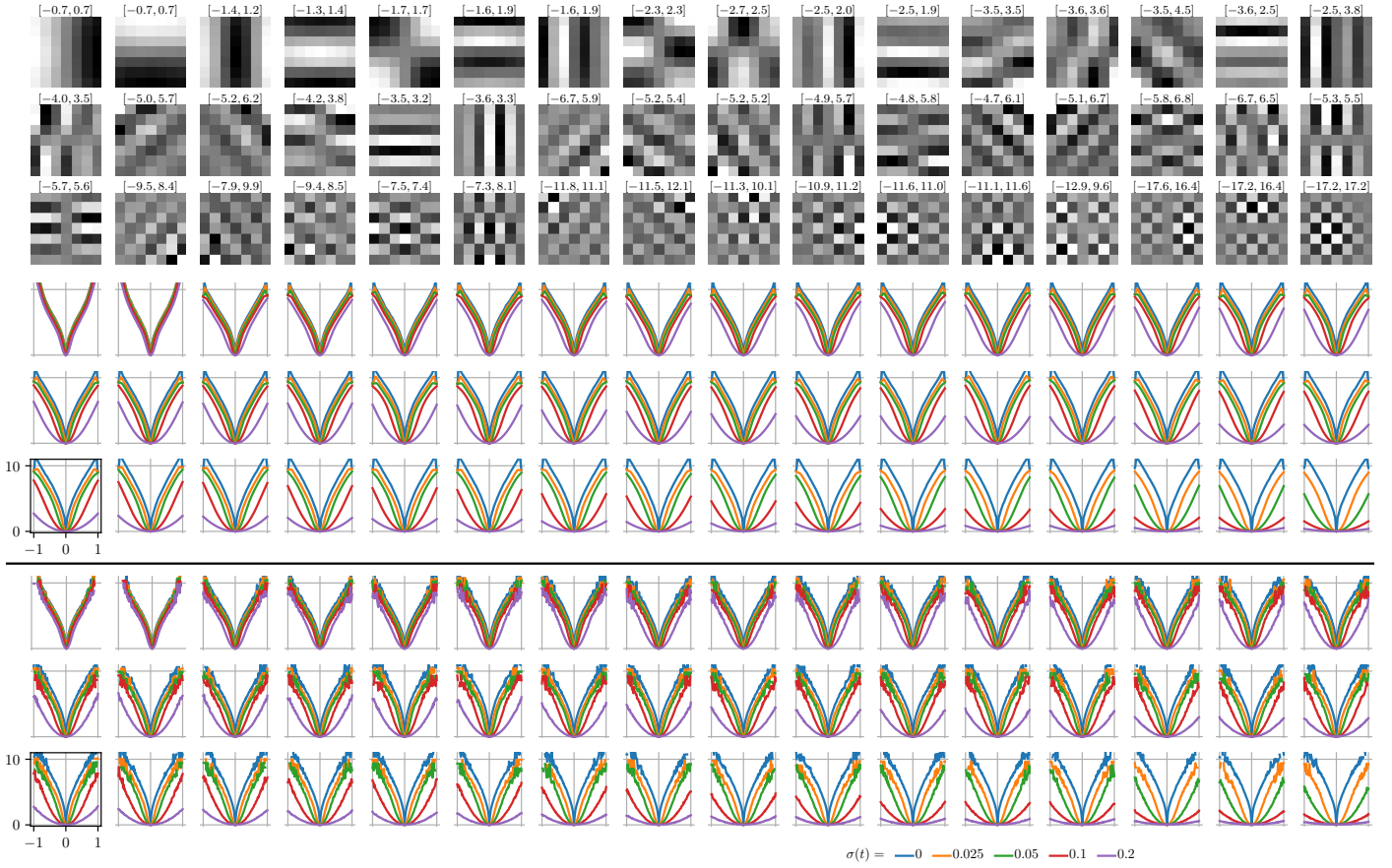


Figure 1: Learned filters k_j (top, the intervals show the values of black and white respectively, amplified by a factor of 10) and potential functions $-\log \psi_j$ (middle). On the bottom the empirical marginal filter response histograms are drawn.

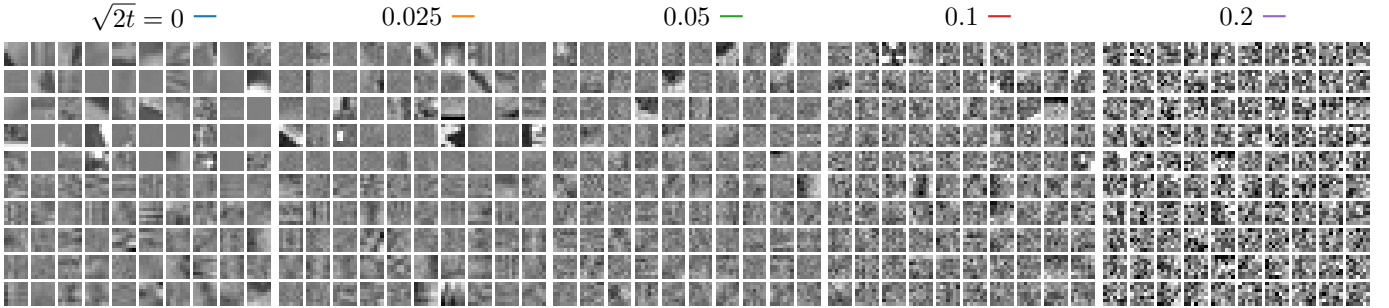


Figure 2: Samples from the random variable Y_t (top) and generated patches (bottom).

Table 1: Quantitative denoising results. Reference numbers are taken from [19].

255 σ	FoE [14]	GMM-EPLL [19]	GMDM ($b = 7 \mid b = 15$)			
			EB-PA		HQS	
15	30.18	31.21	30.00	30.34	30.37	30.69
25	27.77	28.72	27.47	27.81	28.13	28.39
50	23.29	25.72	24.61	24.96	25.32	25.50
100	16.68	23.19	22.14	22.74	23.07	23.12
#Params	648	819200	8352	78400	8352	78400

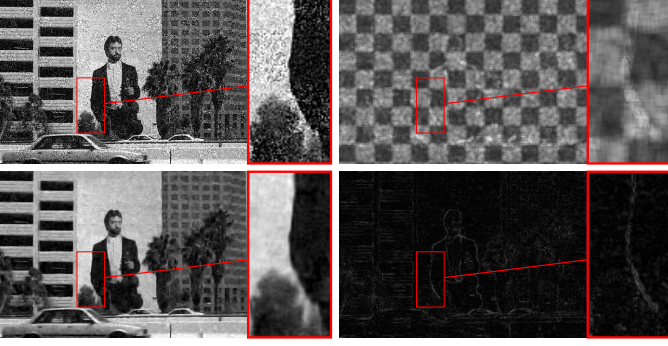


Figure 3: Blind denoising: Image corrupted by heteroscedastic Gaussian noise in a checkerboard-pattern (standard deviation 0.1 and 0.2), noise estimate, EB-PA denoising result, and the difference to the reference image.

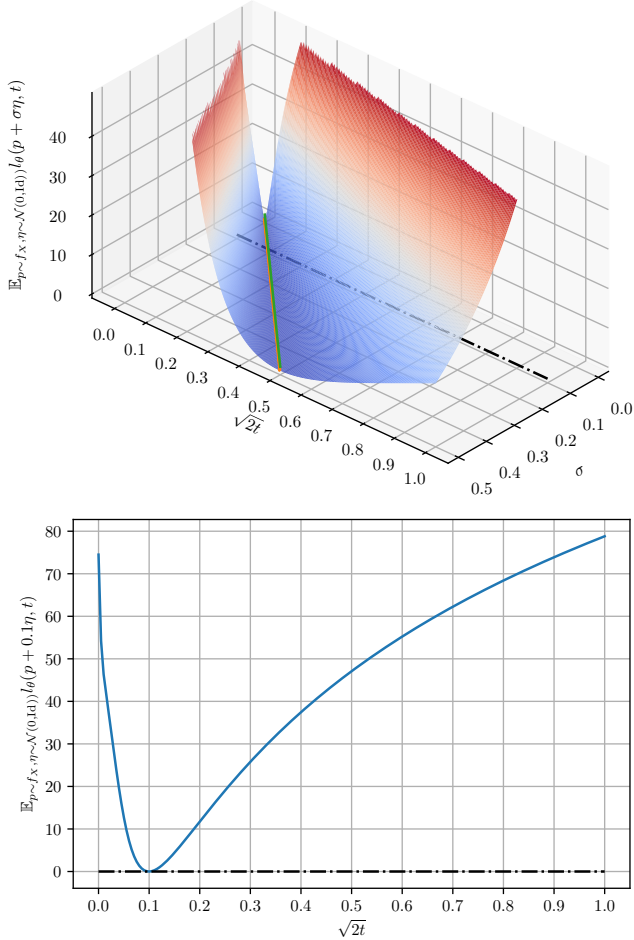


Figure 4: Top: Expected (zero-min-normalized) negative-log density along with the noise estimate — $\sigma \mapsto \arg \min_t \mathbb{E}_{p \sim f_X, \eta \sim \mathcal{N}(0, \text{Id})} l_\theta(p + \sigma \eta, t)$ and — $\sigma \mapsto \sqrt{2t}$. Bottom: The slice at $\sigma = 0.1$.

$U\Sigma V^T$, with U, V in $SO(m), SO(n)$ respectively and Σ $m \times n$ matrices with $\Sigma_{i,j} = 0$ if $i \neq j$, and $\Sigma_{i,i} = \sigma_i \geq 0$ for $i = 1, \dots, n$ (hence if $m = n$ Σ is diagonal, if $m > n$ it is made of a $n \times n$ diagonal matrix “above” a $(m - n) \times n$ null matrix).

The constraints reads $A^T A = V\Sigma^2 V^T$ is diagonal, so that A should have a SVD representation with $V = I$, we assume now it has the form $U\Sigma$.

Then, $\|A - K\| = \|U\Sigma - U^K \Sigma^K (V^K)^T\| = \|(U^K)^T U \Sigma - \Sigma^K (V^K)^T\|$ so without loss of generality, we can assume that K has the form $\Sigma^K (V^K)^T$, and we consider the problem:

$$\min_{U, \Sigma} \|U\Sigma - \tilde{K}\| \quad (22)$$

where $\tilde{K} = \Sigma^K (V^K)^T$. Observe that

$$\|U\Sigma - \tilde{K}\|^2 = \|\Sigma\|^2 - 2(U\Sigma) \cdot \tilde{K} + \|\Sigma^K\|^2$$

The above objective is easily minimized wr Σ or U . For Σ , since $(U\Sigma) \cdot \tilde{K} = \Sigma \cdot (U^T \tilde{K})$ the solution is

$$\sigma_i = (U^T \tilde{K})_{i,i} = \sum_{k=1}^n u_{k,i} \sigma_k^K v_{i,k}^K$$

and the objective becomes (the first term below is constant and could be removed):

$$\min_U \|\Sigma^K\|^2 - \sum_{i=1}^n (U^T \tilde{K})_{i,i}^2.$$

Remark: Frank-Wolfe type method Letting $f(U) := \|\Sigma^K\|^2 - \sum_{i=1}^n (U^T \tilde{K})_{i,i}^2$, one has $\nabla f(U) \cdot M = -2 \sum_{j=1}^n (U^T \tilde{K})_{j,j} (\sum_{i=1}^m M_{i,j} \tilde{K}_{i,j})$, that is

$$(\nabla f(U))_{i,j} = -2(U^T \tilde{K})_{j,j} \tilde{K}_{i,j} = -2\sigma_j \tilde{K}_{i,j}.$$

for $j \leq n$, and 0 for $j > n$. This means that the alternating minimization algorithm can be viewed as a Frank-Wolfe type method on f : starting from $U^0 = I$, one finds U^{n+1} by minimizing $\nabla f(U^n) \cdot U$ for $U \in SO(m)$. A stationary point is clearly a local minimum, yet as f is concave, it is not clear that it is a global minimum.

On the other hand, minimizing wr U means solving

$$\max_{U^T U = I} U \cdot (\tilde{K} \Sigma^T)$$

since $(U\Sigma) \cdot \tilde{K} = \text{Tr } U\Sigma \tilde{K}^T = \text{Tr } U(\tilde{K} \Sigma^T)^T = U \cdot (\tilde{K} \Sigma^T)$.

Now, given M a $m \times m$ matrix, $\max_{O \in SO(m)} O \cdot M = \|M\|_1$ is the sum of the singular values. Indeed if $M = U\Sigma V^T$ with $U, V \in SO(m)$, $O \cdot M = O \cdot (U\Sigma V^T) = (U^T O V) \odot \Sigma$ and the max is reached for $O = UV^T$, with value $\sum_i \sigma_i$.

Hence the problem above is solved for $U = U^\Sigma (V^\Sigma)^T$ where U^Σ, V^Σ are the $m \times m$ orthogonal matrices arising in the SVD representation of $\tilde{K} \Sigma^T$. Then, the objective becomes:

$$\min_{\Sigma} \|\Sigma\|^2 - 2\|\tilde{K} \Sigma^T\|_1 + \|\Sigma^K\|^2$$

Now we show that in fact we can work only with smaller, $n \times n$ matrices, using the particular form of \tilde{K} . Indeed, $(\tilde{K}\Sigma^T)_{i,j} = \sum_{l=1}^n \sum_{k=1}^n \sigma_i^K \delta_{i,l} (V^K)_{k,l} \sigma_k \delta_{j,k}$ is 0 if $i > n$ or $j > n$, and $\sigma_i^K (v^K)_{j,i} \sigma_j$ else. Denoting $(\tilde{K}\Sigma^T)_n$ this reduced $n \times n$ matrix it is obvious that it has the same singular values as $\tilde{K}\Sigma^T$ and hence, the objective can be reduced to

$$\min_{(\sigma_i)_i} \sum_{i=1}^n \sigma_i^2 - 2\|(\sigma_i \sigma_j^K v_{i,j}^K)_{i,j=1}^n\|_1 + \|\Sigma^K\|^2$$

equivalently, we can replace the problem (22) with the same problem, yet with smaller $n \times n$ matrices, and in particular $U \in SO(n)$ instead of $SO(m)$.

Assume now we iterate by alternatively minimizing over U and Σ and suppose we reach a fixed point. Then, consider $f(U) = \|\Sigma^K\|^2 - \sum_{i=1}^n (U^T \tilde{K}_n)_{i,i}^2$ where $\tilde{K}_n = (\sigma_i^K v_{i,j}^K)_{i=1}^n$. One has for small t :

$$\begin{aligned} f(U + tM) &= - \sum_i ((U^T + tM^T) \tilde{K}_n)_{i,i}^2 = - \sum_i (U^T \tilde{K}_n)_{i,i}^2 \\ &\quad - 2t \sum_i (U^T \tilde{K}_n)_{i,i} \left(\sum_j M_{j,i} (\tilde{K}_n)_{j,i} \right) + o(t) \end{aligned} \quad (23)$$

showing that $(\nabla f(U))_{i,j} = -2(U^T \tilde{K}_n)_{j,j} (\tilde{K}_n)_{i,j} = -2\sigma_j (\tilde{K}_n)_{i,j} = -2\tilde{K}_n \Sigma$ (where now $\Sigma = \Sigma^T$ since it is a $n \times n$ diagonal matrix).

Now if M is tangent to $SO(n)$, one has $(U + tM)^T (U + tM) = I + t(M^T U + U^T M) + t^2 M^T M = I + o(t)$ so that $M^T U + U^T M = 0$. Being (U, Σ) a fixed point one has $U = U^\Sigma (V^\Sigma)^T$ where $\tilde{K}_n \Sigma = U^\Sigma D (V^\Sigma)^T$ for some diagonal matrix D . Then,

$$\begin{aligned} \nabla f(U) \cdot M &= -2 \text{Tr}(M^T U^\Sigma D (V^\Sigma)^T) \\ &= -2 \text{Tr}(M^T U V^\Sigma D (V^\Sigma)^T) = 2 \text{Tr}(U^T M V^\Sigma D (V^\Sigma)^T) \\ &= 2 \text{Tr}(M V^\Sigma D (U^\Sigma)^T) = 2 \text{Tr}(M (\tilde{K}_n \Sigma)^T) = -\nabla f(U) \cdot M \end{aligned}$$

so that $\nabla f(U) \cdot M = 0$ and U is a critical point of f on $SO(n)$.

B Additional Experiments

To emphasize the importance of the diffusion for learning, we learn a model solely on $\sigma = 0.02$ and compare the learned potential functions to the empirical marginal filter responses. In detail, Fig. 6 shows the normalized mean-squared error $\text{NMSE}_\kappa : \sqrt{2t} \mapsto \sum_{j=1}^J \int_{\Omega_j(t, \kappa)} \frac{(\psi_j(z, \mathbf{w}_j, t) - h_j(z, t))^2}{\max_{z \in \Omega_j(t, \kappa)} h_j^2(z, t)} dz$. To avoid regions in which the empirical histogram is extremely unreliable, we define a ‘‘credible interval’’ $\Omega_j(t, \kappa) = \{[\alpha, \beta] \subset \mathbb{R} : \int_{-\infty}^\alpha h(\cdot, t) = \int_\beta^\infty h(\cdot, t) = \kappa\}$, and show different $\kappa \in \{0.005, 0.01, 0.02\}$. The results show that training for multiple noise scales improves the performance. In particular, larger diffusion times improve the performance also for (e.g.) $\sigma = 0.02$ especially in low-density regions, which

is apparent when κ is small. When κ is large, we observe that the performance of the models only diverges when σ becomes relatively large.

We show that our model is also scalable by learning on 15×15 patches. The subset containing 112 of the $15^2 - 1$ filters and potential functions shown in Fig. 7 indicate that the results and discussion from the main paper also apply to much larger filter sizes. The model shown in the figure was used in the denoising experiments in Table 1 in the main paper.

References

- [1] Bengio, Y., Courville, A., Vincent, P.: Representation learning: A review and new perspectives. *IEEE Transactions on Pattern Analysis and Machine Intelligence* **35**(8), 1798–1828 (2013)
- [2] Cole, K., Beck, J., Haji-Sheikh, A., Litkouhi, B.: *Heat Conduction Using Greens Functions*. CRC Press (Jul 2010)
- [3] Efron, B.: Tweedie’s formula and selection bias. *Journal of the American Statistical Association* **106**(496), 1602–1614 (2011)
- [4] Gut, A.: *An Intermediate Course in Probability*. Springer New York (2009)
- [5] Hinton, G.E.: Training products of experts by minimizing contrastive divergence. *Neural Computation* **14**(8), 1771–1800 (8 2002)
- [6] Hyvarinen, A.: Estimation of non-normalized statistical models by score matching. *Journal of Machine Learning Research* p. 14 (2005)
- [7] Kirkpatrick, S., Gelatt, C.D., Vecchi, M.P.: Optimization by simulated annealing. *Science* **220**(4598), 671–680 (May 1983)
- [8] Martin, D., Fowlkes, C., Tal, D., Malik, J.: A database of human segmented natural images and its application to evaluating segmentation algorithms and measuring ecological statistics. In: *Proc. ICCV*. vol. 2, pp. 416–423 vol.2 (2001)
- [9] Miyasawa, K.: An empirical bayes estimator of the mean of a normal population. In: *Bulletin of the International Statistical Institute*. pp. 161–188 (1961)
- [10] Pock, T., Sabach, S.: Inertial proximal alternating linearized minimization (iPALM) for nonconvex and nonsmooth problems. *SIAM Journal on Imaging Sciences* **9**(4), 1756–1787 (Jan 2016)
- [11] Raphan, M., Simoncelli, E.P.: Least Squares Estimation Without Priors or Supervision. *Neural Computation* **23**(2), 374–420 (02 2011)

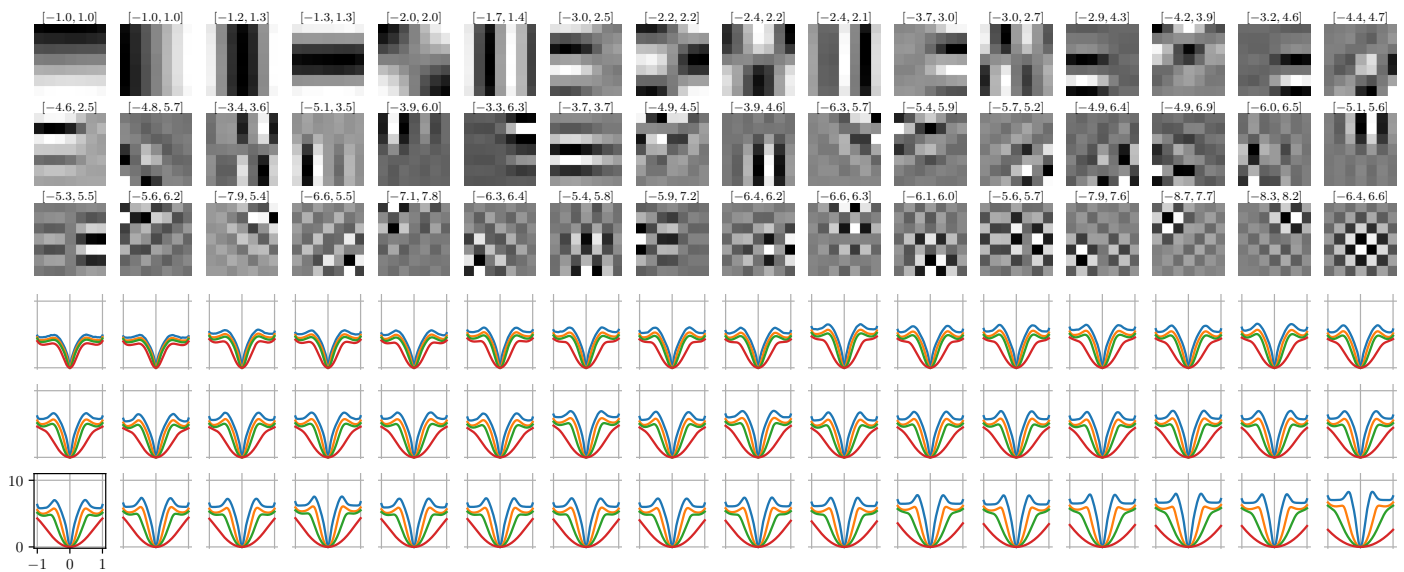


Figure 5: Learned filters k_j (top, the intervals show the values of black and white respectively, amplified by a factor of 10) and potential functions $-\log \psi_j$ (bottom) for a model trained only on $\sigma = 0.02$.

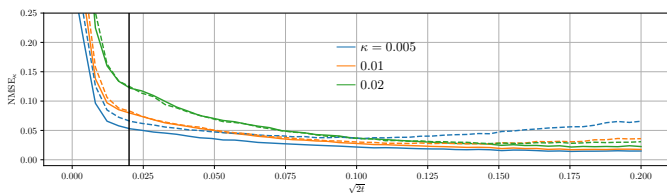


Figure 6: Normalized mean-squared error between the learned potentials and the empirical marginals: For the solid lines, a model was trained on multiple noise scales, whereas only $\sigma = 0.02$ was used for the dashed lines.

through stochastic differential equations. In: International Conference on Learning Representations (2021)

[18] Vincent, P.: A connection between score matching and denoising autoencoders. *Neural Computation* **23**(7), 1661–1674 (2011)

[19] Zoran, D., Weiss, Y.: From learning models of natural image patches to whole image restoration. In: *Proc. of the International Conference on Computer Vision*. pp. 479–486. IEEE (2011)

[12] Robbins, H.: An empirical bayes approach to statistics. In: *Proc. of the Berkeley Symposium on Mathematical Statistics and Probability*. pp. 157–163 (1956)

[13] Roberts, G.O., Tweedie, R.L.: Exponential convergence of langevin distributions and their discrete approximations. *Bernoulli* **2**(4), 341 – 363 (1996)

[14] Roth, S., Black, M.J.: Fields of Experts. *Int. J. Comput. Vis.* **82**(2), 205–229 (2009)

[15] Schrepf, O., Feiermann, O., Hanebeck, U.: Optimal mixture approximation of the product of mixtures. In: *International Conference on Information Fusion*. vol. 1, pp. 8 pp.– (2005)

[16] Song, Y., Ermon, S.: Generative modeling by estimating gradients of the data distribution. In: *Advances in Neural Information Processing Systems*. vol. 32 (2019)

[17] Song, Y., Sohl-Dickstein, J., Kingma, D.P., Kumar, A., Ermon, S., Poole, B.: Score-based generative modeling

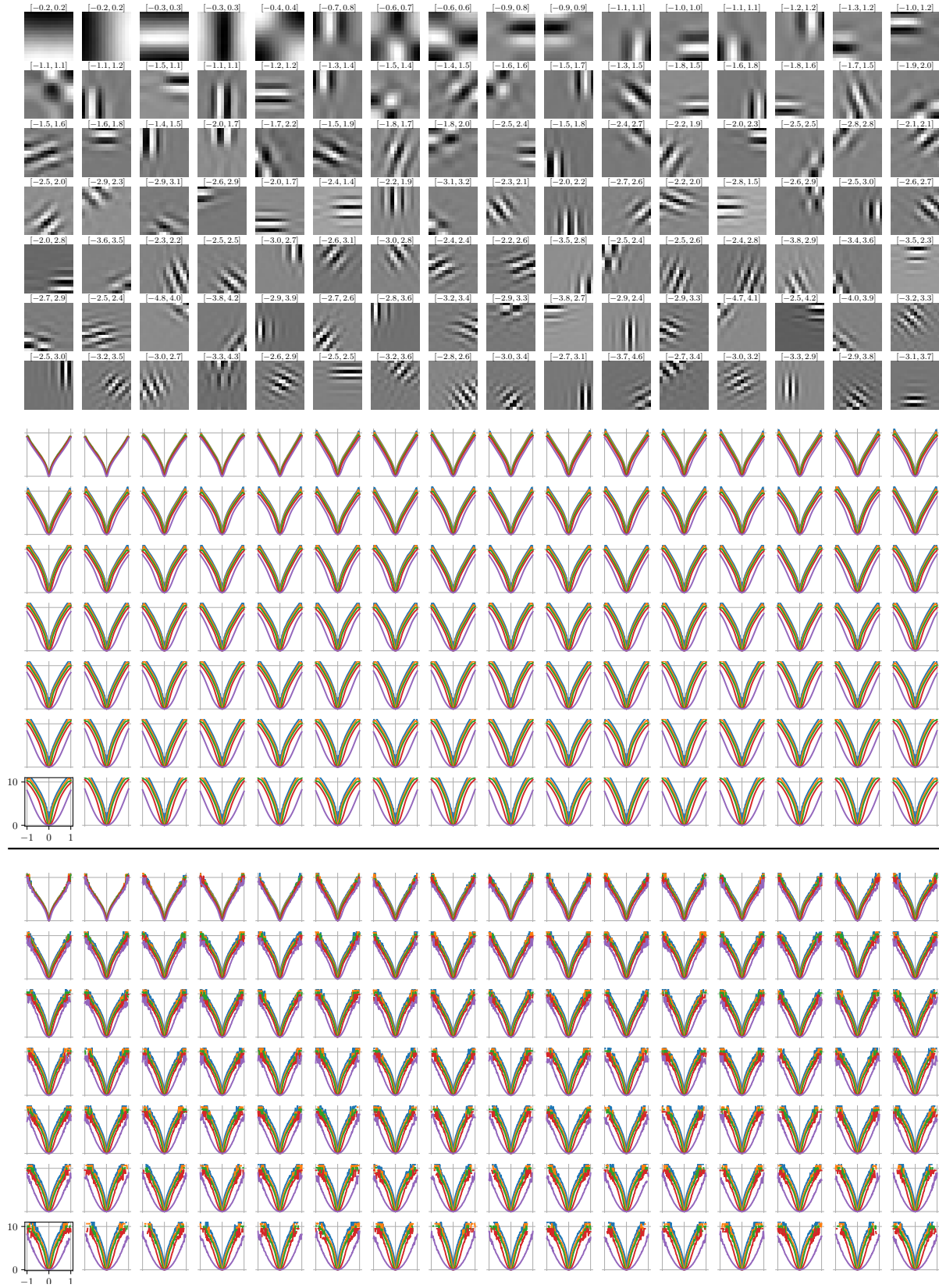


Figure 7: Learned filters k_j (top, the intervals show the values of black and white respectively, amplified by a factor of 10) and potential functions $-\log \psi_j$ (bottom).